

# Dynamic conductivity of semiconducting manganites approaching the metal-insulator transition

**P. Lunkhenheimer\***, **F. Mayr**, and **A. Loidl**

Experimental Physics V, Center for Electronic Correlations and Magnetism, University of Augsburg, 86135 Augsburg, Germany

Received xx Month 2005

**Key words** optical conductivity, ac conductivity, manganites, metal-insulator transition, hopping conductivity.

**PACS** 78.30.-j, 71.30+h, 72.20.Ee

We report the frequency-dependent conductivity of the manganite system  $\text{La}_{1-x}\text{Sr}_x\text{MnO}_3$  ( $x \leq 0.2$ ) when approaching the metal-insulator transition from the insulating side. Results from low-frequency dielectric measurements are combined with spectra in the infrared region. For low doping levels the behavior is dominated by hopping transport of localized charge carriers at low frequencies and by phononic and electronic excitations in the infrared region. For the higher Sr contents the approach of the metallic state is accompanied by the successive suppression of the hopping contribution at low frequencies and by the development of polaronic excitations in the infrared region, which finally become superimposed by a strong Drude contribution in the fully metallic state.

## 1 Introduction

In recent years, the perovskite-related manganites have attracted tremendous interest, mainly triggered by the discovery of the colossal magnetoresistance (CMR) [1]. But these systems, being governed by many competing interactions (superexchange, double exchange, charge ordering, and Jahn-Teller effect) leading to very rich phase diagrams, are also renowned for providing prototypical examples of temperature, doping, and magnetic-field induced metal-to-insulator (MI) transitions. The theoretical [2, 3, 4] and experimental [5, 6, 7, 8, 9, 10, 11, 12, 13, 14, 15, 16, 17, 18] investigation of the dynamical conductivity played a significant role in the clarification of the charge transport processes and the types of charge carriers in these manganites. However, still our understanding of the many puzzling properties of these materials is far from complete and the theoretical understanding of the importance of the electron-phonon coupling [19, 20] has to be verified in optical experiments.. In the present work, we report on the evolution of the dynamic conductivity of the classical CMR manganite  $\text{La}_{1-x}\text{Sr}_x\text{MnO}_3$  ( $0 \leq x \leq 0.2$ ) when approaching the MI transition from the insulating side. Both, dielectric measurements in the Hz-GHz frequency range and optic measurements in the far- to near-infrared range were performed. They provide complementary information giving insight into the mechanisms that are active when the metallic state, hallmarked by a well pronounced Drude contribution, develops out of the insulating one, characterized by strongly localized charge carriers. Our results, together with those obtained on various other transition metal oxides, allow for the development of a general scenario for the evolution of the broadband dynamic conductivity when approaching the metallic state from the insulating side.

$\text{LaMnO}_3$  is a charge-transfer insulator. In the octahedral environment the  $3d$ -levels of the  $\text{Mn}^{3+}$  ions are split into a lower  $t_{2g}$  triplet and an excited  $e_g$  doublet. The  $e_g$  states are filled with one electron and

\* Corresponding author E-mail: Peter.Lunkhenheimer@Physik.Uni-Augsburg.de

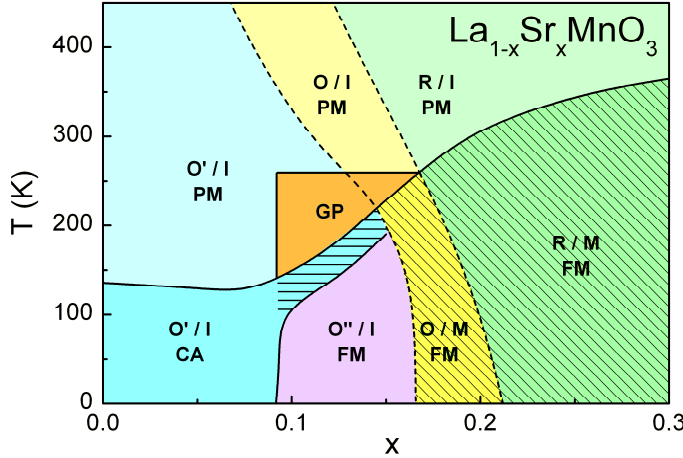


**Fig. 1** The  $(x, T)$  phase diagram of  $\text{La}_{1-x}\text{Sr}_x\text{MnO}_3$  [23, 24, 25, 26]. The structural (O, O', O'', R), magnetic (PM, CA, FM), and electronic (M, I) phases are indicated. The diagonally hatched areas indicate the metallic states. In the horizontally hatched area, electronic phase-separation may exist [24]. "GP" denotes the Griffiths phase, proposed in [25].

hence are strongly Jahn-Teller active. Indeed, below 800 K  $\text{LaMnO}_3$  exhibits orbital order with a half-filled lower and an empty excited  $e_g$  level. On substituting  $\text{La}^{3+}$  by  $\text{Sr}^{2+}$ , holes are introduced into the lower  $e_g$  level, weakening the JT interactions and driving the system into a metallic state [21]. Already in the early days it was speculated that for the metal-to-insulator transition double exchange might play an important role, driving the system from a paramagnetic insulator into a ferromagnetic metal [22].

The rich phase diagram of the  $\text{La}_{1-x}\text{Sr}_x\text{MnO}_3$  system for low doping levels is given in Figure 1, based on dc, magnetic, optic, and electron spin resonance measurements [23, 24, 25, 26]. Depending on doping and temperature, the system exhibits a rhombohedral (R) and three different orthorhombic structures (O, O', O''; see [23, 24, 26] for details). At low concentrations ( $x < 0.1$ ) there is a Jahn-Teller (JT) distorted and insulating orthorhombic phase O', which at low temperatures reveals canted antiferromagnetism (CA). The ground state is an orbitally ordered and ferromagnetic insulator (FM/O''/I) for  $0.1 \leq x \leq 0.15$ , and a FM metal for  $x > 0.17$  in the non-JT distorted O and R phases (diagonally hatched area). Finally, the triangular region, marked "GP", denotes the Griffiths phase, which was postulated in [25], based on electron spin resonance and magnetic measurements. The formation of this phase, which is characterized by ferromagnetic clusters formed below a characteristic temperature  $T_G$  ( $\approx 270$  K in the present case), was ascribed to quenched disorder of the randomly distributed FM bonds in this material [25]. At the FM phase boundary, the clusters achieve FM order and percolate.

## 2 Experimental Details

Well characterized single crystals of  $\text{La}_{1-x}\text{Sr}_x\text{MnO}_3$ , grown by the floating zone method, were kindly provided by Profs. A.A. Mukhin and A.M. Balbashov [27]. Measurements of the dc conductivity were performed using a standard four-point technique. For the non-metallic samples, the ac conductivity at frequencies below 1 GHz was recorded using an autobalance bridge HP4284 covering frequencies  $20 \text{ Hz} \leq \nu \leq 1 \text{ MHz}$  and an HP4291 impedance analyzer at frequencies  $1 \text{ MHz} \leq \nu \leq 1.8 \text{ GHz}$  [28]. The microwave conductivity was measured at 7.3 GHz utilizing a microwave perturbation technique within a  ${}^4\text{He}$ -flow cryostat. In the IR regime the temperature-dependent conductivity was determined via reflectivity measurements using a Bruker IFS 113v Fourier transform spectrometer. From the reflectivity  $R$ , the conductivity  $\sigma'$  was calculated via the Kramers-Kronig transformation, requiring an extrapolation of the data

towards low and high frequencies. For  $\nu \rightarrow 0$ , a constant extrapolation was used for the insulating states and a Hagen-Rubens law for the metallic states. At high frequencies the spectra were extrapolated by a power law  $R \propto \nu^{-1.5}$  up to  $10^6 \text{ cm}^{-1}$ , leading to a smooth transition to the experimental data, which was followed by a  $\nu^{-4}$  power law at higher frequencies [29]. For some samples, additional measurements at 7.3 GHz and around 100 GHz were performed using a microwave perturbation technique and a quasi-optic Mach-Zehnder spectrometer [30], respectively.

### 3 Results and Discussion

In Fig. 2 the frequency dependent reflectivity of  $\text{La}_{1-x}\text{Sr}_x\text{MnO}_3$  is shown for four doping levels up to  $x = 0.2$ . The sharp resonance features showing up in the region between 100 and  $1000 \text{ cm}^{-1}$  (3 - 30 THz) are due to phonon excitations. They are most prominent in the insulating regions of the phase diagram, i.e. for the low doping levels shown in Figs. 2(a) and (b) and for the higher temperatures at the higher doping levels given in Figs. 2(c) and (d). For a detailed discussion of these phonon modes the reader is referred to references [15, 23, 29, 31, 32, 33, 34, 35, 36, 37]. For the insulating states, immediately following the last phonon mode the reflectivity increases sharply with increasing frequency. This can be ascribed to the onset of electronic excitations across a band gap, which at higher frequencies leads to a peak in the reflectivity close to  $10^4 \text{ cm}^{-1}$  ( $\approx 1.3 \text{ eV}$ ). Above about  $2 \times 10^4 \text{ cm}^{-1}$ , the onset of a further electronic excitation is observed for all doping levels shown in Fig. 2. It is clear from the electronic structure of the doped manganites that below  $10^4 \text{ cm}^{-1}$  excitations between and within the JT-split  $e_g$  levels dominate. The charge-transfer gap, corresponding to a transition between the oxygen  $2p$ - and the manganese  $e_g$  states, is expected close to  $4 \text{ eV} \approx 3 \times 10^4 \text{ cm}^{-1}$  and is just covered at the high-frequency end of the reflectivity spectra for all compounds shown in Fig. 2. For the metallic sample with  $x = 0.2$  [Fig. 2(d)] and when the metallic state is approached with decreasing temperature at for  $x = 0.175$  [Fig. 2(c)], the gaplike excitations below  $10^4 \text{ cm}^{-1}$  and the phonon modes are superimposed by a strong additional contribution, smoothly increasing and finally tending to saturate with decreasing frequency. These are the characteristic features of a Drude contribution due to free charge carriers.

To gain deeper insight into the various processes contributing to the infrared reflectivity and to relate the results to those obtained at sub-GHz frequencies, it is helpful to calculate the frequency dependent conductivity from the reflectivity using the Kramers-Kronig transformation. Figure 3 shows the frequency dependence of  $\sigma'$  of pure  $\text{LaMnO}_3$  at selected temperatures, combining results at low frequencies [11] and in the infrared region [29]. Only those parts of the spectra are shown that are not affected by contact contributions [38], which were shown in [11] to dominate at very low frequencies and high temperatures. As already noted in [11], for  $\nu < 1 \text{ GHz}$ , three contributions can be identified: For  $\nu \rightarrow 0$ ,  $\sigma'$  approaches the frequency-independent dc conductivity. Its temperature dependence follows the prediction of the Variable-Range-Hopping model [11]. With increasing frequency,  $\sigma'$  increases smoothly, which can be parameterized by a sublinear power law  $\sigma' \propto \nu^s$  with  $s < 1$  [11], a behavior termed "Universal Dielectric Response" (UDR) due to its universal occurrence in a variety of materials [39]. Such a behavior is commonly regarded as a hallmark feature of hopping conduction of charge carriers subjected to disorder-induced localization [40]. Superimposed to this power law, a shoulder shows up at low temperatures. As revealed by the upper inset of Fig. 3, it corresponds to well-pronounced peaks in the dielectric loss  $\varepsilon'' \propto \sigma'/\nu$  shifting through the frequency window with temperature. This is typical for a relaxational process, which was ascribed to localized hopping of polarons in [11]. However, it should be noted that the energy barrier of 86 meV, determined from the temperature dependence of the relaxation time [11], obviously has no relation to the energy scales of the polaronic excitations observed in the infrared region, which are discussed below.

It is not possible to extrapolate the sublinear power law found below GHz towards the infrared results in the THz regime, even if assuming  $s = 1$  as indicated by the dash-dotted line in Fig. 3. Clearly an additional contribution must be present in the so-far uninvestigated intermediate region. We propose that there is an additional superlinear power law (SLPL),  $\sigma' \propto \nu^n$ , with  $n \approx 1.2$  as indicated by the dashed line. Such a

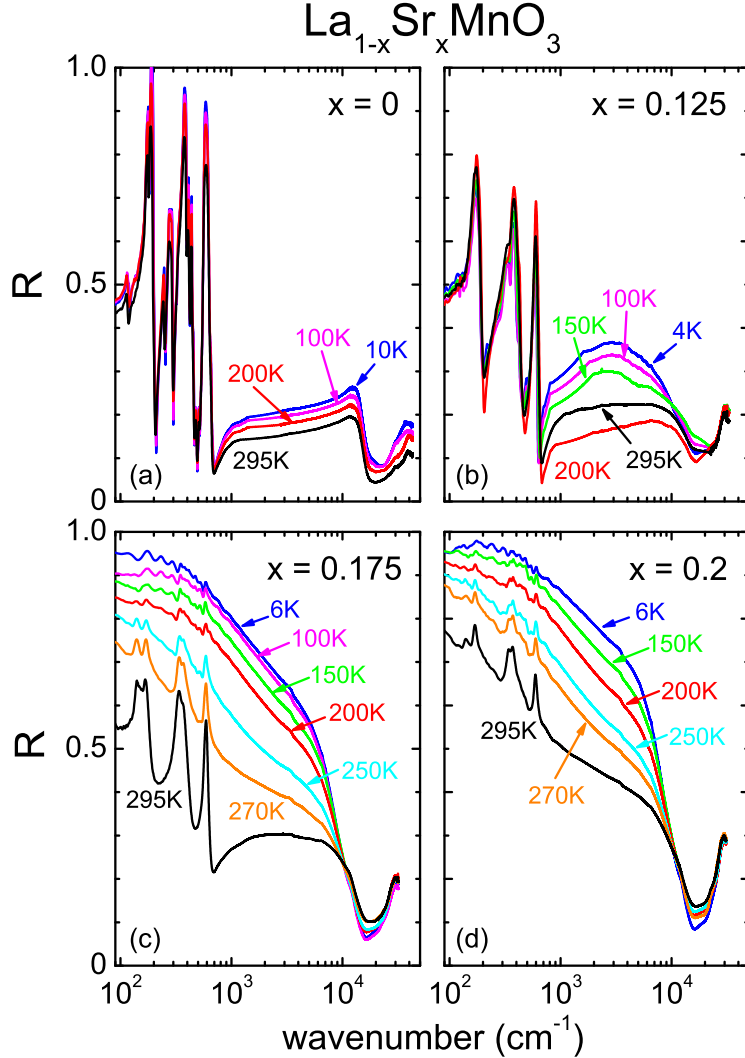


**Fig. 2** Frequency dependent infrared reflectivity of  $\text{La}_{1-x}\text{Sr}_x\text{MnO}_3$  for four different doping levels and various temperatures.

SLPL was clearly detected, e.g., in the CMR manganite  $\text{Pr}_{0.65}(\text{Ca}_{0.8}\text{Sr}_{0.2})_{0.35}\text{MnO}_3$  [16] and evidenced to be a universal feature of disordered matter [41], e.g. supercooled liquids or doped semiconductors. In the present case of a nominally undoped material without any substitutional disorder, a slight off-stoichiometry or impurities at the ppm level seem to be sufficient to produce this typical response of disordered matter, as it is also the case, e.g., for  $\text{LaTiO}_3$  [42].

In the infrared region, at frequencies beyond the phonon resonances a peak shows up at about 380 THz, corresponding to 1.6 eV. As shown in the lower inset of Fig. 3, its peak frequency is nearly independent of temperature. This peak most probably corresponds to an electronic transition between the JT-split  $e_g$  bands. The excitation from one  $e_g$  orbital to another at the same site is forbidden and should have negligible oscillator strength. Hence, this peak structure must correspond to a transition between Mn-ions on adjacent sites, which, due to Hund's coupling, is favorable for parallel spin alignment. Thus, at first glance

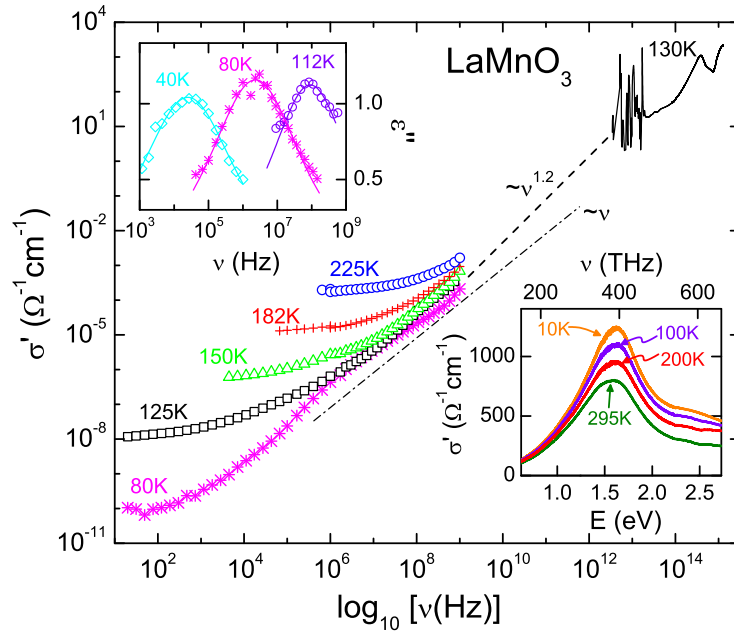


**Fig. 3** Frequency dependent conductivity of  $\text{LaMnO}_3$  at sub-GHz and infrared frequencies for various temperatures. The upper inset shows the dielectric loss below GHz; the lines are fits with the empirical Cole-Cole function [11]. The lower inset shows  $\sigma'$  in the region of the electronic excitation close to 1.5 eV for various temperatures.

at the magnetic phase transition an anomaly in the intensity is expected, but experimentally only a moderate temperature dependence is observed (lower inset of Fig. 3). This finding may be explained considering that in the paramagnetic phase the spins are thermally disordered while in the type-A antiferromagnetic state, order is established with ferromagnetic spin alignment within and antiferromagnetic order between the  $(a,b)$ -planes. But the above interpretation is not corroborated by polarized light-scattering experiments, which indicate a strong charge-transfer character of this transition [17]. Further experiments will be necessary to unravel the nature of this transition.

In Fig. 4, reproduced from ref. [23], the frequency-dependent conductivity of  $\text{La}_{0.875}\text{Sr}_{0.125}\text{MnO}_3$  is shown for three temperatures. At room temperature, where the dc conductivity is rather high, the low-frequency measurements provide information on the intrinsic conductivity in a restricted frequency range only, because at low frequencies the contact contributions and at high frequencies the inductance of the sample dominates [11]. Nevertheless, from Fig. 4 it seems clear that in the sub-GHz range the room-temperature conductivity is frequency independent. However, interpolating from GHz to the lowest frequencies of the FIR experiment, thereby taking into account the single point at 7.3 GHz from a microwave resonance measurement, it seems likely that in this region a small increase of  $\sigma'(\nu)$  is present. It can be suspected to be caused by hopping conduction of localized charge carriers, the corresponding sublinear power law emerging from the dc background with increasing frequency. The presence of this contribution, pointing to a localization of the charge carriers also in this compound, becomes even more obvious at the lower temperatures, where a succession of a clearly pronounced sublinear power law and a SLPL can be suspected. The non-metallic character of this compound is further corroborated by the complete absence of a Drude contribution in the infrared region. Instead, above the phonon modes, the conductivity exhibits a strong increase, which can be ascribed to superposed contributions from polaron absorption and interband transitions, as discussed in detail in [15, 29].

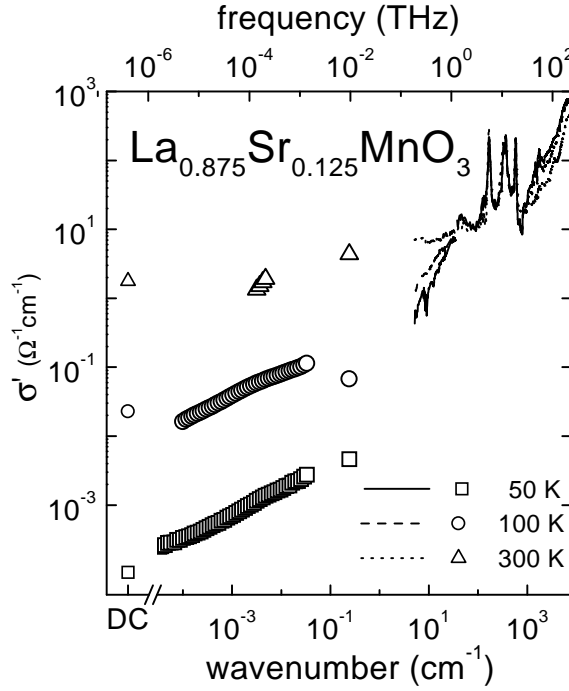


**Fig. 4** Frequency dependent conductivity of  $\text{La}_{0.875}\text{Sr}_{0.125}\text{MnO}_3$  at three temperatures. In addition, the results of a four-point dc-measurement are indicated. (reproduced from [23])

For Sr contents  $x = 0.175$  and  $0.2$ , having ferromagnetic metallic ground states, the measured low-frequency conductivity is dominated by inductance and skin effect contributions [11]. The intrinsic  $\sigma'(\nu)$  can be expected to reveal a significant frequency dependence only at high frequencies, in the infrared and optical region, as shown in Fig. 5. For  $x = 0.175$ , at high temperatures, where the sample is close to the MI transition (cf. Fig. 1),  $\sigma'(\nu)$  shows a broad peak at about  $10^4 \text{ cm}^{-1}$ . With decreasing temperature, spectral weight is shifted from this excitation towards lower frequencies, leading to a peak or shoulder strongly shifting towards lower frequencies when the sample becomes more metallic with decreasing temperature. Finally, at  $6 \text{ K}$   $\sigma'$  increases markedly towards low frequencies, in good accord with the strongly enhanced dc conductivity, thus exhibiting the clear signature of a Drude contribution of free charge carriers. A detailed analysis of the Drude response in  $\text{La}_{0.825}\text{Sr}_{0.175}\text{MnO}_3$  was provided in [13]. It seems reasonable to assume that the excitation at about  $11000 \text{ cm}^{-1}$  or  $1.4 \text{ eV}$  has a similar origin as that at  $1.6 \text{ eV}$  for pure  $\text{LaMnO}_3$ . But now we have a fraction of  $\text{Mn}^{4+}$  sites with no  $e_g$  electrons. Hence, in addition to transitions between JT-split  $e_g$  orbitals, optical transitions between empty and occupied  $e_g$  levels have to be taken into account. We believe that the broad peak at room temperature at  $1.4 \text{ eV}$  is a mixture of both processes. With decreasing temperatures a remainder of the JT-split derived peak still is visible at  $1.4 \text{ eV}$ , indicating the significantly weaker JT energy in the doped crystals compared to the  $1.6 \text{ eV}$  observed in the pure compound (Fig. 3). The second spectral feature branching off from this excitation and being strongly temperature dependent can be ascribed to a polaronic excitation. Similar behavior has been reported in [5] exemplifying the importance of strong electron-phonon interactions in the manganites. The strong softening of this polaronic excitation qualitatively resembles the behaviour predicted by Millis [3] for a scenario of strong electron-phonon coupling. However, in the case of half-filling, the polaronic excitation transforms into a Drude type behavior at low temperatures. In  $\text{La}_{1-x}\text{Sr}_x\text{MnO}_3$  ( $0 \leq x \leq 0.2$ ) a Drude peak evolves with doping simultaneously with the polaronic excitation, with the Drude peak being characterized by a low relaxation rate and a very low optical weight. The rather symmetric shape of the polaron peak

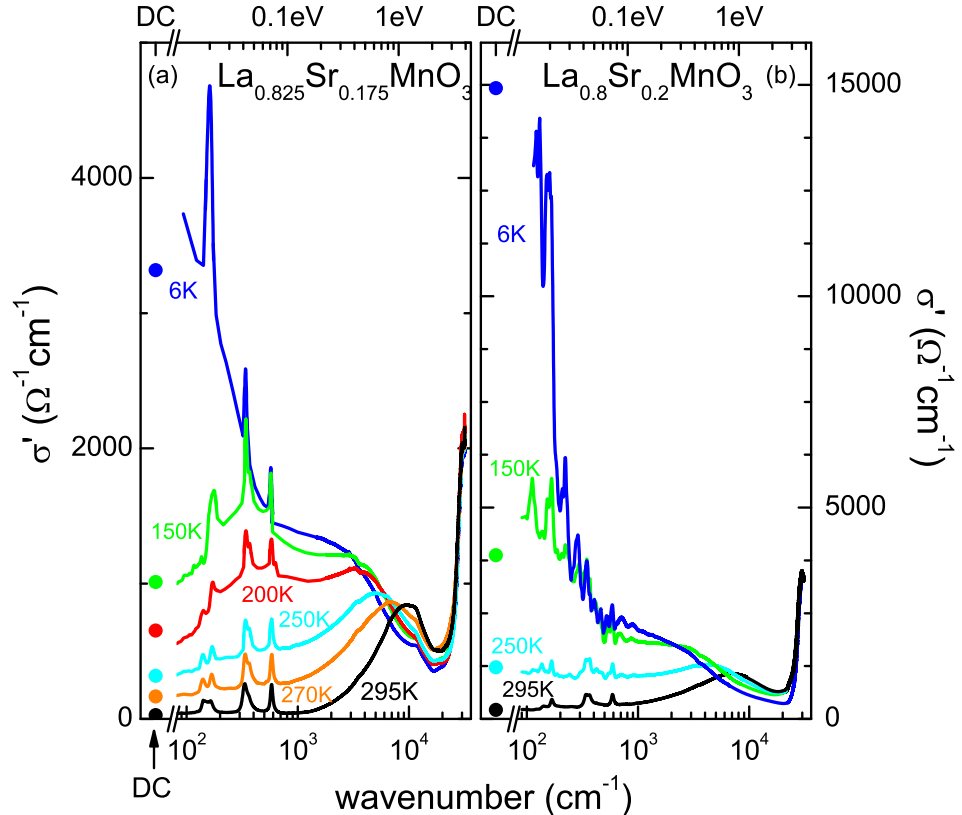


**Fig. 5** Frequency dependent conductivity of  $\text{La}_{1-x}\text{Sr}_x\text{MnO}_3$  for  $x = 0.175$  and  $0.2$  at various temperatures. In addition, the results of a four-point dc-measurement are indicated.

with the absence of a clear cut-off frequency at low frequencies indicates the dominance of small polarons [18]. Finally, at the high-frequency edge of the investigated spectral range, a further strong increase of the conductivity shows up, indicating the onset of the charge-transfer excitation as in pure  $\text{LaMnO}_3$ . For  $x = 0.2$  [Fig. 5(b)], the overall behavior is qualitatively similar to that observed for  $x = 0.175$ . However, the excitation ascribed to the polaronic transition seems to be shifted to lower energy, now located at about  $0.8$  eV at room temperature and of significantly lower optical weight. At the lowest temperatures a narrow Drude peak dominates the optical conductivity and the polaronic excitation appears as a weak shoulder close to  $3000$  cm<sup>-1</sup>.

In Fig. 6, a least-square fit of the conductivity of  $\text{La}_{0.825}\text{Sr}_{0.175}\text{MnO}_3$  measured at  $6$  K is shown (dashed line). For the fit, the sum of a Drude term dominating at low frequencies and a Lorentz term (peak frequency  $\nu_0 = 2040$  cm<sup>-1</sup>, damping constant  $\gamma = 7180$  cm<sup>-1</sup>) taking into account the polaronic excitation was used. The three phonon modes were neglected. A good description of the experimental data could be achieved in this way, revealing a Drude relaxation time of  $\tau = 1.8 \times 10^{-14}$  s. Using a Fermi velocity for the orthorhombic structure of  $2.2 \times 10^7$  cm/s [43], we obtain a mean free path of  $4$  nm, which characterizes this compound as a bad metal. As discussed earlier, the symmetric form of the polaron absorption points towards the existence of small polarons [18]. The small ratio of the optical weight of the Drude conductivity to that of the polaron absorption (Fig. 6) indicates that only a small fraction of free charge carriers contributes to the Drude-like conductivity, while the majority still is localized by strong electron-phonon coupling effects.

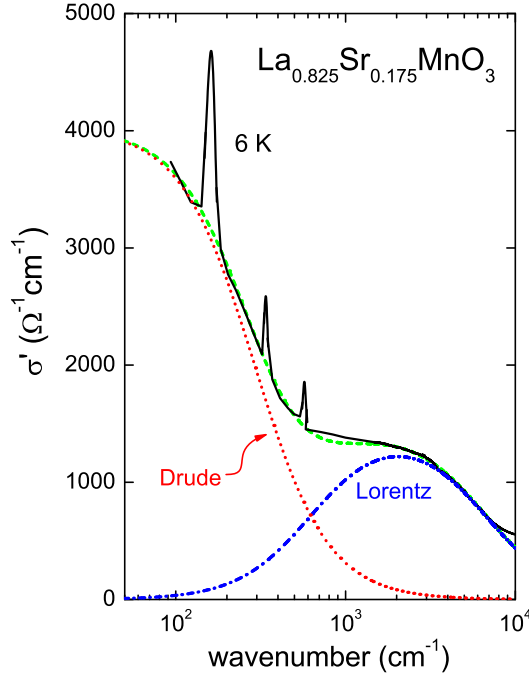


**Fig. 6** Frequency dependent conductivity of  $\text{La}_{0.825}\text{Sr}_{0.175}\text{MnO}_3$  at 6 K (solid line). The dashed line is a fit of the experimental spectrum using the sum of a Drude and a Lorentz term. These two contributions are indicated by the dotted and dash-dotted lines, respectively.

#### 4 Summary and Conclusions

The ac conductivity of the CMR manganite  $\text{La}_{1-x}\text{Sr}_x\text{MnO}_3$  was reported for four doping levels  $x$ . The combination of low-frequency and optical measurements revealed the importance of hopping conduction of localized charge carriers for the non-metallic parts of the phase diagram of this system. In the infrared region beyond the phonon modes, evidence for two electronic modes were obtained, one of them showing the clear signature of a polaronic excitation. Deep in the metallic state a strong Drude contribution is observed.

Taking together the results of the present work and those obtained on a variety of further transition metal oxides and other systems being close to a MI transition [11, 16, 41, 42, 44], allows for the development of a general scenario for the broadband ac conductivity when approaching the MI transition from the insulating side. As schematically indicated in Fig. 7, deep in the insulating phase most materials show a succession of a dc plateau, a sublinear, and a superlinear power law [41]. Such a behavior seems to be closely connected to hopping conduction of charge carriers that are localized due to disorder. One should note, however, that this notion is mainly based on theories that were developed for amorphous or heavily doped conventional semiconductors [40, 45] and whose predictions can be approximated by a sublinear power law. It is not clear, if these theories also should be applicable to electronically correlated materials as, e.g., the CMR manganites. Also so far there is no well-founded explanation for the SLPL, which seems to occur concomitantly with the sublinear law. Whatsoever, it seems clear now that in the insulating and semiconducting states these power laws are also active in the only rarely investigated transition region between the classical dielectric frequencies ( $\sim$  below GHz) and those of typical infrared experiments. Often

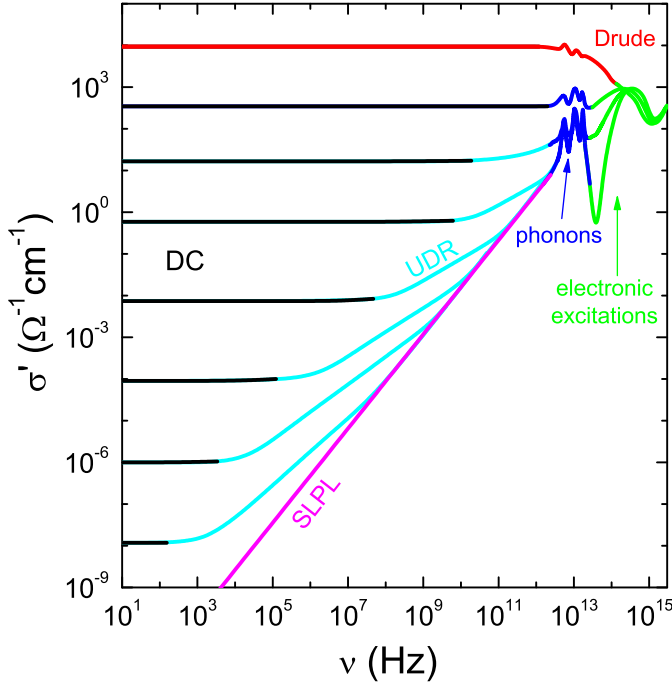


**Fig. 7** Schematic plot of the conductivity of a system approaching a MI transition from the insulating side as observed, e.g., in transition metal oxides. The figure covers a broad range, starting at frequencies of typical dielectric experiments up to those covered by optical spectrometers. The lowest curves correspond to the most insulating, the highest to the most metallic states. The values of the tick labels are intended to give a rough estimate only.

they even seem to represent the background for the phonon modes, however, vanishing abruptly beyond the highest phonon resonance. When the system further approaches the metallic state, the dc conductivity, growing more rapidly than the UDR and the nearly constant SLPL, dominates over an increasingly broader frequency range, which finally extends well up to the first phonon modes (second curve from above in Fig. 7). This typically occurs for a dc conductivity of about  $100 - 1000 \Omega^{-1} \text{cm}^{-1}$  and marks the transition into the metallic state. Up to this point, the infrared response is dominated by strong phonon modes, followed by electronic excitations due to interband and polaronic contributions. Within the metallic phase, the phonons and low-lying electronic modes are successively superimposed by the typical free carrier Drude behavior as indicated by the uppermost curve in Fig. 7. It is interesting that the value of  $\sigma'$  marking the transition from insulating to a Drude-like metallic behavior seems to be rather universal and a connection of this finding to the concept of the "minimum metallic conductivity" proposed by Mott [46] may be suspected.

**Acknowledgements** We thank A.A. Mukhin and A.M. Balbashov for providing the samples and A. Pimenov, K. Pucher, and A. Seeger for performing part of the measurements. Stimulating discussion with Th. Kopp and Ch. Hartinger are gratefully acknowledged. This work was supported by the Deutsche Forschungsgemeinschaft via the Sonderforschungsbereich 484 and by the BMBF via VDI/EKM.

## References

[1] K. Chahara, T. Ohno, M. Kasai, and Y. Kozono, *Appl. Phys. Lett.* **63**, 1993 (1993); R. von Helmolt, J. Wecker, B. Holzapfel, L. Schultz, and K. Samwer, *Phys. Rev. Lett.* **71**, 2331 (1993); S. Jin, T. H. Tiefel, M. McCormac,

R. A. Fastnacht, R. Ramesh, and L. H. Chen, *Science* **264**, 413 (1994).

[2] N. Furukawa, *J. Phys. Soc. Japan* **64**, 3164 (1995).

[3] A. J. Millis, B. I. Shraiman, and R. Mueller, *Phys. Rev. B* **77**, 175 (1996); A. J. Millis, R. Mueller, and B. I. Shraiman, *Phys. Rev. B* **54**, 5389 (1996); A. J. Millis, R. Mueller, and B. I. Shraiman, *Phys. Rev. B* **54**, 5405 (1996).

[4] P. Horsch, J. Jaklic, and F. Mack, *Phys. Rev. B* **59**, 6217 (1999); F. Mack and P. Horsch, *Phys. Rev. Lett.* **82**, 3160 (1999).

[5] Y. Okimoto *et al.*, *Phys. Rev. Lett.* **75**, 109 (1995); Y. Okimoto *et al.*, *Phys. Rev. B* **55**, 4206 (1997).

[6] S. G. Kaplan *et al.*, *Phys. Rev. Lett.* **77**, 109 (1996).

[7] J. H. Jung *et al.*, *Phys. Rev. B* **55**, 15489 (1997).

[8] J. H. Jung *et al.*, *Phys. Rev. B* **59**, 3793 (1999); J. H. Jung *et al.*, *Phys. Rev. B* **57**, R11043 (1998); H. J. Lee *et al.*, *Phys. Rev. B* **60**, 5251 (1999); K. H. Kim *et al.*, *Phys. Rev. Lett.* **81**, 4983 (1998); K. H. Kim, S. Lee, T. W. Noh, and S.-W. Cheong, *Phys. Rev. Lett.* **88**, 167204 (2002).

[9] M. Quijada *et al.*, *Phys. Rev. B* **58**, 16093 (1998).

[10] A. Machida, Y. Moritomo, and A. Nakamura, *Phys. Rev. B* **58**, R4281 (1998).

[11] A. Seeger *et al.*, *J. Phys.: Condens. Matter* **11**, 3273 (1999).

[12] Y. Okimoto *et al.*, *Phys. Rev. B* **59**, 7401 (1999); E. Saitoh *et al.*, *Phys. Rev. B* **60**, 10362 (1999).

[13] K. Takenaka, Y. Sawaki, and S. Sugai, *Phys. Rev. B* **60**, 13011 (1999).

[14] A. Paolone *et al.*, *Eur. Phys. J. B* **16**, 245 (2000).

[15] F. Mayr *et al.*, *Phys. Rev. B* **62**, 15673 (2000).

[16] J. Sichelschmidt *et al.*, *Eur. Phys. J. B* **20**, 7 (2001).

[17] K. Tobe, T. Kimura, Y. Okimoto, and Y. Tokura, *Phys. Rev. B* **64**, 184421 (2001).

[18] Ch. Hartinger, F. Mayr, J. Deisenhofer, A. Loidl, and Th. Kopp, *Phys. Rev. B* **69**, 100403(R) (2004).

[19] A. J. Millis, P. B. Littlewood, and B. I. Shraiman, *Phys. Rev. Lett.* **74**, 5144 (1995); A. J. Millis, *Phys. Rev. B* **53**, 8434 (1996).

[20] H. Röder, Jun Zang, and A. R. Bishop, *Phys. Rev. Lett.* **76**, 1356 (1996).

[21] G. H. Jonker and J. H. van Santen, *Physica* **16**, 337 (1950).

[22] P. G. de Gennes, *Phys. Rev.* **118**, 141 (1960).

[23] M. Paraskevopoulos *et al.*, *J. Mag. Mag. Mat.* **211**, 118 (2000).

[24] M. Paraskevopoulos *et al.*, *J. Phys.: Condens. Matter* **12**, 3993 (2000).

[25] J. Deisenhofer *et al.*, cond-mat/0501443.

[26] J. Hemberger *et al.*, *Phys. Rev. B* **66**, 66, 094410 (2002).

[27] A. M. Balbashov, S. G. Karabashev, Y. M. Mukovskiy, and S. A. Zverkov, *J. Cryst. Growth* **167**, 365 (1996); A. A. Mukhin, V. Y. Ivanov, V. D. Travkin, S. P. Lebedev, A. Pimenov, A. Loidl, and M. Balbashov, *JETP Lett.* **69**, 356 (1998).

[28] U. Schneider *et al.*, *Ferroelectrics* **249**, 89 (2001).

[29] F. Mayr, Breitbandige optische Spektroskopie an Manganaten mit Perowskit-Struktur, Ph.D. thesis, (Shaker, Aachen, 2003).

[30] B. Gorchunov, A. A. Volkov, A. Mukhin, M. Dressel, S. Uchida, and A. Loidl, *Int. J. Infrared and Millimeter Waves* **26**, 1217 (2005).

[31] K. H. Kim *et al.*, *Phys. Rev. Lett.* **77**, 1877 (1996).

[32] I. Fedorov *et al.*, *Phys. Rev. B* **60**, 11875 (1999).

[33] M. V. Abrashev *et al.*, *Phys. Rev. B* **59**, 4146 (1999).

[34] A. Paolone *et al.*, *Phys. Rev. B* **61**, 11255 (2000).

[35] Ch. Hartinger, F. Mayr, A. Loidl, and Th. Kopp, *Phys. Rev. B* **70**, 134415 (2004).

[36] Ch. Hartinger, F. Mayr, A. Loidl, and Th. Kopp, *Phys. Rev. B* **71**, 184421 (2005).

[37] F. Mayr, Ch. Hartinger, and A. Loidl, *Phys. Rev. B* **72**, 024425 (2005).

[38] P. Lunkenheimer *et al.*, *Phys. Rev. B* **66**, 052105 (2002).

[39] A. K. Jonscher, *Nature* **267**, 673 (1977).

[40] A. R. Long, *Adv. Phys.* **31**, 553 (1982); S. R. Elliott, *Adv. Phys.* **36**, 135 (1987); M.P. J. van Staveren, H.B. Brom and L. J. de Jongh, *Phys. Rep.* **208**, 1 (1991).

[41] P. Lunkenheimer and A. Loidl, *Phys. Rev. Lett.* **91**, 207601 (2003).

[42] P. Lunkenheimer *et al.*, *Phys. Rev. B* **68**, 245108 (2003).

[43] D. J. Singh and W. E. Pickett, *Phys. Rev. B* **57**, 88 (1998).

[44] P. Lunkenheimer, M. Resch, A. Loidl, and Y. Hidaka, *Phys. Rev. Lett.* **69**, 498 (1998); M. Dumm *et al.*, *Eur. Phys. J. B* **6**, 317 (1998); A. I. Ritus *et al.*, *Phys. Rev. B* **65**, 165209 (2002); P. Lunkenheimer, R. Fichtl, S. G. Ebbinghaus, and A. Loidl, *Phys. Rev. B* **70**, 172102 (2004).

[45] M. Pollak and T. H. Geballe, *Phys. Rev.* **122**, 1742 (1961); I. G. Austin and N. F. Mott, *Adv. Phys.* **18**, 41; (1969); S. R. Elliott, *Phil. Mag.* **36**, 1291 (1977).

[46] N. F. Mott and E. A. Davis, *Electronic Processes in Non-Crystalline Materials* (Clarendon Press, Oxford, 1979).